

Resonance induced by a bound state in the continuum in a two-level nonlinear Fano-Anderson model

Evgeny N. Bulgakov and Almas F. Sadreev

Institute of Physics, Russian Academy of Sciences, 660036 Krasnoyarsk, Russia

(Received 25 May 2009; revised manuscript received 29 July 2009; published 10 September 2009)

We consider the transmission through a nonlinear media in the framework of a two-level nonlinear Fano-Anderson model. The model is realized in photonic crystal waveguide coupled with two off-channel defects with the instantaneous Kerr-type nonlinearity. We reveal a resonance and argue that it is a result of excitement of bound state in the continuum (BSC) by transmitted wave. The resonance induced by BSC is located at the energy of BSC with a width proportional to the amplitude of incident wave. The BSC exists at any distance between energy levels of the two-level nonlinear Fano-Anderson model that is fundamentally different from the linear case.

DOI: [10.1103/PhysRevB.80.115308](https://doi.org/10.1103/PhysRevB.80.115308)

PACS number(s): 05.60.Gg, 42.25.Bs, 42.65.Pc

I. INTRODUCTION

Resonances are signatures of bound states which eventually decay into the continuum coupled to them. There are many examples of resonances in different branches of physics, but basically they are classified as the symmetric Breit-Wigner and the asymmetric Fano resonances in the linear quantum systems. In this paper we consider a type of the resonance in nonlinear system, which is trace of the bound state in the continuum (BSC). First, the BSC as discrete localized solutions of the single-particle Schrödinger equation embedded in the continuum of positive-energy states was predicted in 1929 by Neumann and Wigner.¹ Their analysis examined by Stillinger and Herrick² was long time regarded as mathematical curiosity because of certain spatially oscillating central symmetric potentials. However in 1977 Herrick³ and Stillinger⁴ predicted BSCs in semiconductor heterostructure superlattices observed by Capasso *et al.* as a very narrow absorption peak.⁵ In the last time the phenomenon of BSC attracted large interest in application to different systems,⁶⁻⁸ in particular in highly promising photonic crystals.⁹⁻¹²

It is easy to understand the BSC phenomenon using the Feshbach theory of resonances.¹³ If two resonances pass each other as the function of a continuous physical parameter, then for a certain value of the parameter one resonance will have an exactly vanishing width.^{14,15} The resonance width vanishes as a result of that the coupling constant of the resonance state with the continuum disappears because of destructive interference.¹⁵ In a series of papers¹⁴⁻¹⁷ BSC was considered analytically in the framework of the standard two-level Fano-Anderson model (FAM) (Refs. 18 and 19), which describes the interaction of two impurity states $|n\rangle, n=1, 2$ with the continuum. Although the model is exclusively simple, it can be applied to any physical system which justifies the two-level approximation. The Hamiltonian of the total system is $H=H_B+H_C+V$, where H_B given by a diagonal matrix describes the impurity bound states and H_C describes the extended states of the continuum. V is responsible for the interaction between the bound states and the extended ones. The total Hilbert space is separated into the intrinsic part and the continuum, and the continuum part can be eliminated

with the aid of projection operators.^{13,20,21} Then the Lippmann-Schwinger (LS) equation after projection onto the intrinsic part of the Hilbert space takes the following form:^{20,21}

$$(E - H_{eff})|\psi\rangle = i\hat{V}\phi_{in}, \quad (1)$$

where

$$H_{eff} = H_B - i\hat{V}\hat{V}^+ = \begin{pmatrix} E_1 - i\Gamma_1 & i\sqrt{\Gamma_1\Gamma_2} \\ i\sqrt{\Gamma_1\Gamma_2} & E_2 - i\Gamma_2 \end{pmatrix} \quad (2)$$

is the non-Hermitian effective Hamiltonian and $\hat{V}^+ = (\sqrt{\Gamma_1}\sqrt{\Gamma_2}\dots)$ describes coupling of the impurity states with the continuum. In the two-level approximation the LS equation becomes

$$\begin{aligned} (E - E_1 + i\Gamma_1)A_1 + i\sqrt{\Gamma_1\Gamma_2}A_2 &= \sqrt{\Gamma_1}\phi_{in}, \\ i\sqrt{\Gamma_1\Gamma_2}A_1 + (E - E_2 + i\Gamma_2)A_2 &= \sqrt{\Gamma_2}\phi_{in}, \end{aligned} \quad (3)$$

where $E_{1,2} = \mp \omega_0$ are the eigenenergies of the impurity, ϕ_{in} is the amplitude of an incident wave, and

$$|\psi\rangle = A_1|1\rangle + A_2|2\rangle. \quad (4)$$

Equations (3) formulate the Fano-Anderson model of the wave transmission through two-level impurity embedded in the one-channel continuum. With the accuracy of notations, Eqs. (3) coincide with coupled-mode equations^{22,23} describing photonic waveguides with defects. In what follows we take for simplicity $\Gamma_1 = \Gamma_2 = \Gamma$ without loss of generality.

The solution of the LS equation is given by the inverse of the matrix $(E - H_{eff})$. However, there might be the special case when the inverse does not exist. It is easy to see that it happens at $\omega_0 = 0$ and $E = 0$. By the use of the complex eigenvalues $z_{1,2} = -i\Gamma \pm \sqrt{-\Gamma^2 + \omega_0^2}$ of H_{eff} , which give positions [via $\text{Re}(z)$] and widths of the resonance states [via $\text{Im}(z)$],²⁰ we obtain that at the point $\omega_0 = 0$ one resonance becomes an infinitely narrow width [$\text{Im}(z_1) = 0$] while the second one acquires the maximal width 2Γ .¹⁴⁻¹⁶ As a result the transmission probability accompanies by collapse of the Fano resonance²⁴ for $\omega_0 = 0$.

At the point $E=0$, $\omega_0=0$, there is the homogeneous solution of the LS equation (1) $\frac{1}{\sqrt{2}}\begin{pmatrix} 1 \\ -1 \end{pmatrix} = |\psi_{BSC}\rangle$ for $\phi_{in}=0$. If a quantum particle were at this state, it never would decay into the continuum because of the ideal interference at leads. The particle remains localized at the impurity states and, therefore, is the BSC.²⁵ As known from linear algebra, the necessary and sufficient condition for the existence of the inhomogeneous solution of the LS equations (1) for $\phi_{in} \neq 0$ is that the vector $\langle \psi_{BSC} |$ is to be orthogonal to the incoming vector $\phi_{in}\begin{pmatrix} 1 \\ 1 \end{pmatrix}$. It holds indeed. Then the general solution of Eq. (1) at the BSC point can be given by^{5,17}

$$|\psi\rangle = \alpha |\psi_{BSC}\rangle + \frac{\phi_{in}}{\sqrt{2}} \begin{pmatrix} 1 \\ 1 \end{pmatrix}, \quad (5)$$

where α is an arbitrary coefficient and the second term is the particular transport solution of Eq. (1). The orthogonality of the BSC to incoming wave $\phi_{in}\hat{V}$ implies that the BSC is not coupled to the continuum and cannot be excited by incoming wave, and therefore there is no resonance at their discrete energy $E_c=0$ for the linear transmission.

We argue that is *not the case* for the nonlinear Anderson impurity. A nonlinearity violates the principle of superposition, i.e., Eq. (5), and thereby the incoming wave couples with the BSC. In the linear systems the BSC is rather a subtle phenomenon because it occurs only at the isolated point $\omega_0=0$. We show below that in the nonlinear two-level FAM the BSC exists in a whole range of ω_0 .

II. TIGHT-BINDING MODEL OF THE NONLINEAR DEFECTS COUPLED TO THE LINEAR CHAIN

We consider the photonic crystal in the form of a two-dimensional square lattice array of parallel axis dielectric cylinders (consisted of linear dielectric medium) in vacuum, and defects and waveguides created by cylinder replacement. The waveguide is formed from linear dielectric media, but the off-channel features that it interacts with may be formed from either linear or Kerr nonlinear dielectric media. Waveguide transmission resonances, associated with resonant scattering from electromagnetic modes on the off-channel nonlinear features, were studied in many papers.^{26–30} We consider a discrete model that describes a linear chain of particles coupled to a couple of single-site defects with instantaneous Kerr nonlinearity.

The theoretical approach based on a difference equation formulation for fields in the two-dimensional waveguide channels and off-channel nonlinear impurities coupled to the waveguide was developed in Refs. 26, 27, and 31. The simplest model is a discrete tight-binding model that describes a linear chain of sites coupled to a single-site defect with instantaneous Kerr nonlinearity.^{27,28} It was shown that this model can be regarded as a nonlinear generalization of the single-level Fano-Anderson model and it can generate amplitude-dependent bistable resonant transmission or reflection. Similar effects were shown by McGurn³¹ also as for an off-channel cavity comprised of the single-site defect as for the off-channel cavity composed of many neighboring sites having different Kerr dielectric properties. In the

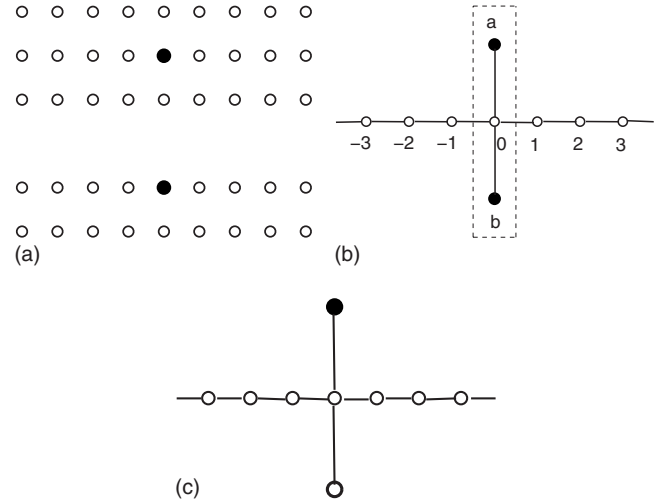


FIG. 1. (a) Photonic crystal consists of a square lattice of dielectric rods with dielectric constant ϵ_0 . A single row of rods is extracted to form one-dimensional directed waveguide. Two nonlinear defect rods made from a Kerr media marked by filled circles are inserted into the photonic crystal. (b) The tight-binding version of the system in (a) with linear chain and two nonlinear defects. (c) One of the defects is linear while the second one is nonlinear.

present paper we consider a similar system which consists of the linear waveguide coupled with two nonlinear off-channel defects as shown in Figs. 1(a)–1(c). We show that this model can be regarded as a nonlinear generalization of the two-level Fano-Anderson model. It can generate not only amplitude-dependent bistable resonant transmission or reflection but also shows resonance induced by the BSC.

We present the waveguide as the simplest tight-binding linear chain coupled at the site $n=0$ with two different nonlinear off-channel defects. Following Miroshnichenko *et al.*,²⁸ we write the Hamiltonian of the tight-binding model for the case in Fig. 1(b) as follows:

$$H = - \sum_n \psi_n \psi_{n+1}^* - u \psi_0 \phi_a^* - u \psi_0 \phi_b^* + \omega_a |\phi_a|^2 + \omega_b |\phi_b|^2 + \text{H.c.}, \quad (6)$$

where $\omega_a = \omega_{a0} + \lambda_a |\phi_a|^2$ ($a=1,2$). If the defects are identical, $\omega_a = \omega_b$, the system of three sites shown in Fig. 1(c) by dashed line has the following eigenstates:

$$|1\rangle = \begin{pmatrix} 1/2 \\ 1/\sqrt{2} \\ 1/2 \end{pmatrix}, \quad |2\rangle = \begin{pmatrix} 1/\sqrt{2} \\ 0 \\ -1/\sqrt{2} \end{pmatrix}, \quad \begin{pmatrix} -1/2 \\ 1/\sqrt{2} \\ -1/2 \end{pmatrix} \quad (7)$$

with the corresponding eigenfrequencies $-\sqrt{2}u, 0, \sqrt{2}u$. The second eigenstate has a node at the second site “0” at which the system is connected to the chain waveguide. Therefore, that state is not coupled with the waveguide forming the BSC with discrete energy $E_c=0$ which occurs for $\omega_a = \omega_b$.

In order to calculate the transmission, we write $\psi_n = \phi_{in} e^{ikn} + r e^{-ikn}$ if $n \leq 0$, and $\psi_n = t \phi_{in} e^{ikn}$ if $n \geq 0$, where ϕ_{in} is the amplitude of incident wave. Then $|r|^2 / \phi_{in}^2$ and $|t|^2 / \phi_{in}^2$ are the reflection and the transmission probabilities, respec-

tively. Resuming calculations in Ref. 28, we immediately obtain the following formulas for the transmission amplitude t :

$$t = \frac{i\phi_{in}}{i + \alpha_k \left[\frac{1}{\omega - \omega_1} + \frac{1}{\omega - \omega_2} \right]}, \quad (8)$$

and for the amplitudes at the defects

$$\phi_a = \frac{ut}{\omega - \omega_a}, \quad \phi_b = \frac{ut}{\omega - \omega_b}, \quad (9)$$

where $\alpha_k = \frac{u^2}{2 \sin k}$.

Equations (9) can be rewritten as follows:

$$\begin{aligned} (\omega - \omega_a + i\alpha_k)\phi_a + i\alpha_k\phi_b &= -iu\phi_{in}e^{ik}, \\ (\omega - \omega_b + i\alpha_k)\phi_b + i\alpha_k\phi_a &= -iu\phi_{in}e^{ik}. \end{aligned} \quad (10)$$

Assume $u \ll 1$, i.e., the eigenfrequencies of the defects are much less in comparison to the width of the propagation band of the chain $\omega_k = -2 \cos k$. Then we can approximate $k \approx \pi/2$ and reduce Eq. (10) to the coupled mode equations (3) with $\Gamma^2 = \alpha_k \approx u^2/2$ provided that the direct coupling of the defects is ignored. The index of the defects a, b can be taken as the index of the energy level $n=1, 2$. As was considered in Refs. 12, 27, and 28, the single-site defects a and b with instantaneous Kerr nonlinearity have the frequencies $\omega_n = \omega_{n0} + \lambda_n |\phi_n|^2$ ($n=1, 2$). Therefore, in notations of Eqs. (3) we can introduce a nonlinearity in the two-level FAM by a substitution

$$E_{1,2} = \mp \omega_0 + \lambda_{1,2} |A_{1,2}|^2 \quad (11)$$

instead of former eigenenergies $E_{1,2}$ in the LS equations (3). That nonlinearity is not general but is typical for the photonic crystal waveguide coupled with defects made from a Kerr-like nonlinear material.²³ It preserves the stationary solution of the Schrödinger equation; however, it violates the principle of linear superposition. Thus, we obtained an explicit analog of Eq. (11) if we take $\omega_{n0} = \mp \omega_0$.

III. TRANSMISSION IN FRAMEWORK OF NONLINEAR TWO-LEVEL FANO-ANDERSON MODEL

As was established in the previous section the system of two nonlinear off-channel defects can be described by the nonlinear FAM provided that (i) the eigenfrequencies are close to center of the propagation band and (ii) we can neglect direct coupling of the defects. Assume that the continuum supports an arbitrary amplitude of the incident wave ϕ_{in} . Similar to the scattering matrix in quantum mechanics,¹⁶ we define a matrix

$$\begin{pmatrix} r & t' \\ t & r' \end{pmatrix} = \begin{pmatrix} \phi_{in} & 0 \\ 0 & \phi_{in} \end{pmatrix} - i\hat{V}^+ \frac{\phi_{in}}{E - H_{eff}} \hat{V}. \quad (12)$$

Let us take $r' = r$, $t' = t$ where t, t' and r, r' are the amplitudes of right and left transmitted and left and right reflected waves, respectively. From Eq. (12) it follows that $|t|^2 + |r|^2$

$= |\phi_{in}|^2$, where $r = \phi_{in} + t$. From Eqs. (3) we obtain

$$\begin{aligned} A_{1,2} &= \frac{\sqrt{\Gamma} \phi_{in} (\tilde{E} \mp \epsilon)}{\tilde{E}^2 - \epsilon^2 + 2i\Gamma\tilde{E}}, \\ t &= \sqrt{\Gamma} (A_1 + A_2), \end{aligned} \quad (13)$$

where

$$\begin{aligned} \tilde{E} &= E - \frac{1}{2}\lambda_1 X - \frac{1}{2}\lambda_2 Y, \quad \epsilon = \omega_0 - \frac{1}{2}\lambda_1 X + \frac{1}{2}\lambda_2 Y, \\ X &= |A_1|^2, \quad Y = |A_2|^2. \end{aligned} \quad (14)$$

Substituting Eqs. (13) into Eqs. (14), we obtain the following nonlinear self-consistent equations:

$$\begin{aligned} X[(\tilde{E}^2 - \epsilon^2)^2 + 4\Gamma^2\tilde{E}^2] &= P(\tilde{E} - \epsilon)^2, \\ Y[(\tilde{E}^2 - \epsilon^2)^2 + 4\Gamma^2\tilde{E}^2] &= P(\tilde{E} + \epsilon)^2, \end{aligned} \quad (15)$$

which are the system of nonlinear algebraic equations because of Eqs. (14). X, Y are the populations of energy levels of the two-level impurity. Or, in view of the tight-binding model considered in the previous section, X, Y are the intensities of the transmitted wave at the off-channel defects. The value $P = \Gamma |\phi_{in}|^2$ is proportional to the input wave power.

Let us first consider a more simple case $\lambda_1 \neq 0, \lambda_2 = 0$, i.e., one of the defects is linear [Fig. 1(c)]. This case preserves the main feature of transmission in the two-level nonlinear FAM as another resonance, but it reduces the self-consistent equations (15) to the fifth-order polynomial of X . Remind the reader that the case of single off-channel nonlinear defect gives the third-order polynomial of X .²⁸ Therefore, the presence of the second defect, even linear, is important and gives rise to other branches as we show below. Examples of the transmission probability $T = |t|^2 / |\phi_{in}|^2$ as dependent on the incident energy (frequency) and on the incident amplitude are shown in Fig. 2. The left resonance undergoes the typical amplitude-dependent bistable resonant transmission observed early^{27,28,32} with the growth of P while the right resonance does not change because of $\lambda_2 = 0$.

The most intriguing result is a resonance shown in Fig. 2(a) by the red line that is located at $E = \omega_0$ for $\lambda_2 = 0$. However, for both off-channel nonlinear defects ($\lambda_1 \neq 0, \lambda_2 \neq 0$), it might be located anywhere at $E > 0$ [see below Figs. 5(a), 6(a), and 6(b)]. As seen from these figures the form of another resonance is rather unusual. Figure 3 shows the solution $X = |A_1|^2$ of the self-consistent equations (15) for $\lambda_2 = 0$. For the small enough input wave power ($P = 0.1$ and $P = 0.6$), there are two distinctive branches of the solution for X . The first lower branch is responsible for the bistability of the left resonance peak shown in Fig. 2(a), which takes place for the single-level FAM too.^{27,28} The second upper branch for X in the form of ‘‘8’’ gives rise to another resonance. With further growth of the input power P , branches are coalesced resulting in a complicated behavior of the transmission as shown in Fig. 2(b).

We argue now that this resonance is related to the BSC. As for the linear case we define the BSC as the solution of the LS equations (3), which exists for zero input wave ϕ_{in}

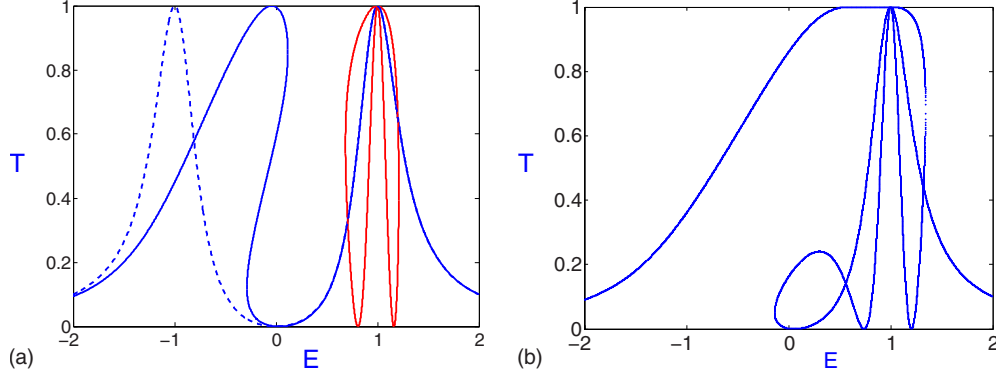


FIG. 2. (Color online) The transmission probability $T=|t|^2/|\phi_{in}|^2$ versus incident energy E for $\omega_0=1$ and $\Gamma=0.25$. The nonlinear parameters are $\lambda_1=0.1$ and $\lambda_2=0$. (a) Dashed line shows the transmission probability for the linear case, solid blue line corresponds to $P=0.6$, and solid red line shows the resonance induced by BSC. (b) $P=1$.

$=0$. It occurs if one of the complex eigenvalues of the matrix $H_{eff}-E$ equals zero. At this point $\tilde{E}=0$, $\epsilon=0$, and the solution of Eq. (3) takes $A_1=-A_2$ for $\phi_{in}=0$.

Then from Eq. (14) we immediately obtain that $X_c=Y_c$ and

$$X_c = \frac{2\omega_0}{\lambda_1 - \lambda_2}, \quad E_c = \frac{1}{2}(\lambda_1 + \lambda_2)X_c = \omega_0 \frac{\lambda_1 + \lambda_2}{\lambda_1 - \lambda_2}, \quad (16)$$

where values X_c and Y_c are the mean-squared amplitudes of the BSC solution. At the BSC point, the eigenenergies (11) become degenerated $E_1=E_2$ because of nonlinear contributions irrespective to the former distance $2\omega_0$. For the particular case $\lambda_2=0$ shown in Figs. 2–4, we obtain from Eq. (16) that the energy of BSC $E_c=\omega_0$. For the parameters given in Fig. 2, one can see that the other resonance is just located at this point. The value of population $X_c=2\omega_0/\lambda_1$ also coincides with that shown in Fig. 3. As the input power $P \rightarrow 0$ the second branch of the solution for X shrinks up to the isolated point X_c at $E=E_c$ noted in Fig. 3 as the point BSC.

Although the transmission through the two-level FAM could be calculated only numerically, we present here analytical estimations for the width of the BSC induced resonance. First, consider the case of $\lambda_1 \neq 0$, $\lambda_2=0$ shown in Fig. 2(a). Then we can evaluate the width by zeros of the transmission

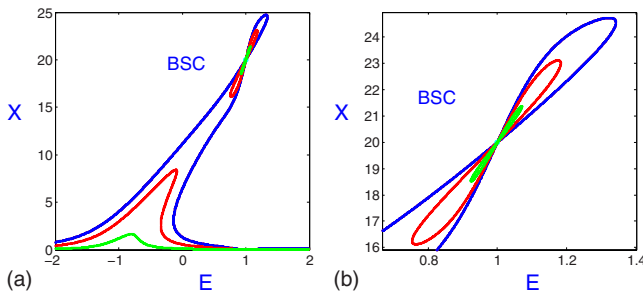


FIG. 3. (Color online) (a) The solution of Eq. (15) for the parameters given in Fig. 2 for $P=0.1$ (green line), $P=0.6$ (red line), and $P=1$ (blue line). (b) Blowup near the vicinity of the BSC point.

$$T = \frac{4\Gamma^2 \tilde{E}^2}{(\tilde{E}^2 - \epsilon^2)^2 + 4\Gamma^2 \tilde{E}^2} \quad (17)$$

at the energies

$$E_c \pm \sqrt{\frac{2P\lambda_1}{\omega_0}}. \quad (18)$$

This formula was obtained from Eqs. (13) for $\tilde{E}=0$, from Eqs. (15), and for P small enough. Therefore, we have an estimate for the BSC induced resonance $\Gamma_{BSC} \sim (P\lambda_1/\omega_0)^{1/2}$. If we take the limit $\lambda_1 \rightarrow 0$, then the width of the BSC resonance tends to zero, while the population X_c goes to infinity that makes the BSC resonance unobservable for the linear limit. Figure 4 demonstrates that one of the resonance widths given by the imaginary part of the complex eigenvalues of the effective Hamiltonian equal to $z_{1,2} = -\Gamma \pm \sqrt{-\Gamma^2 + \epsilon^2}$ turns to zero at $E=E_c=\omega_0$ in full correspondence to the results of the theory of BSC in the linear two-level FAM.^{16,17}

The phenomenon that the BSC becomes observable for the nonlinear case can be traced as follows. At the BSC point the effective Hamiltonian (2) has the following eigenstates: $\begin{pmatrix} 1 \\ -1 \end{pmatrix}$ and $\begin{pmatrix} 1 \\ 1 \end{pmatrix}$ with corresponding eigenvalues $z_{1,2}=0, -2i\Gamma$.¹⁷

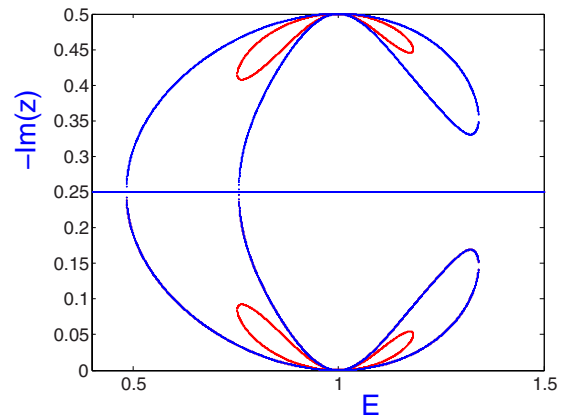


FIG. 4. (Color online) The energy behavior of resonance widths for the parameters of nonlinear FAM given in Fig. 2 for $P=0.5$ (red line) and $P=1$ (blue line).

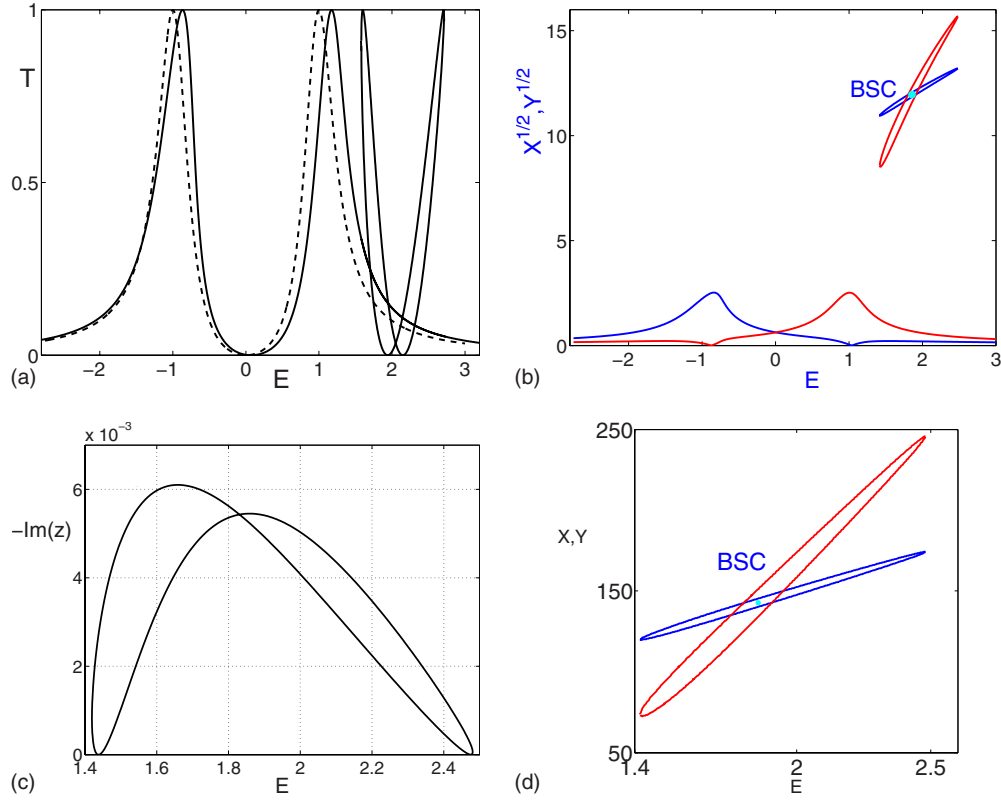


FIG. 5. (Color online) (a) The transmission probability as dependent on energy for $\lambda_1=0.02$, $\lambda_2=0.006$, $\Gamma=0.25$, $\omega_0=1$, and $P=0.4$. Dash line shows the linear case. (b) The numerical solution of the self-consistent equations (15) where blue line corresponds to X and green line corresponds to Y . (c) The behavior of the resonance width. (d) Blowup of (b) near the BSC point.

The first eigenstate which is BSC has a coupling constant with the continuum $i\epsilon/\sqrt{2}\Gamma$ equal to zero at the BSC point $\epsilon=0$, $\tilde{E}=0$. In the linear case the equation $\epsilon=\omega_0=0$ remains irrespective to variation in energy to preserve zero coupling constant of BSC with the continuum. However, for the nonlinear case when the energy differs from E_c the coupling constant becomes nonzero. As a result the incoming wave “sees” the BSC and populates it via the nonlinearity. That conclusion fully correlates with the energy behavior of the resonance width shown in Fig. 4.

Figures 5 and 6 show the case when both nonlinear coefficients differ from zero. The energies of the BSC equal $E_c = 1.86$ for the case in Fig. 5 and $E_c = 3.857$ for the case in Fig. 6, respectively. Obviously, the positions of BSC induced resonance do not coincide with the positions of linear resonances $\mp\omega_0$. Next, the populations of each state, X and Y , of the two-level Anderson impurity are different as shown in Fig. 5(b). As a result the BSC resonance is split. In order to evaluate a value of the splitting, let us find points at which the transmission probability (17) reaches a unit. Obviously, it does at $\tilde{E} = \pm\epsilon$. Substituting these relations into Eqs. (15), we obtain $E_{1,2} = \mp\omega_0 + \lambda_{1,2}P/\Gamma^2$. These energies correspond to the usual peaks of the linear transmission at the energies $\mp\omega_0$ but shift because of nonlinearity. The second case of $T \rightarrow 1$ shown in Figs. 4(a) and 4(d) is not so obvious and can be established for the limit $\tilde{E} \rightarrow 0$, $\epsilon \rightarrow 0$. Then we can con-

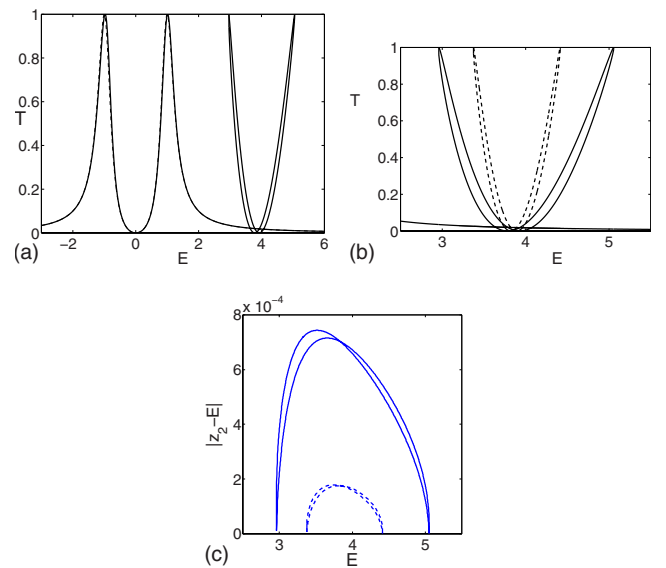


FIG. 6. (Color online) (a) The transmission probability as dependent on energy for $\lambda_1=0.017$, $\lambda_2=0.01$, $\Gamma=0.25$, $\omega_0=1$, $P=0.1$, and $E_c=3.857$. (b) Blowup of the BSC induced resonance for the different input power $P=0.1$ (solid line) and $P=0.0025$ (dash line). (c) The behavior of the resonance $|z_2 - E|$, where $z_2 = -i\Gamma + \sqrt{-\Gamma^2 + \epsilon^2}$ is the complex eigenvalue of the effective Hamiltonian.

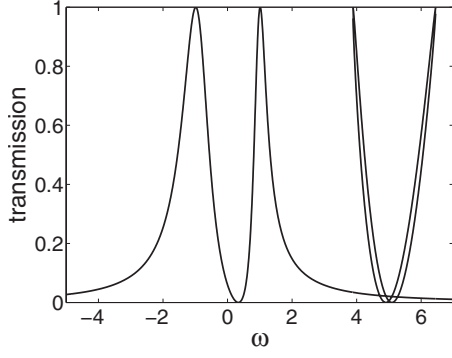


FIG. 7. The transmission $T=|t|^2/|\phi_{in}|^2$ over frequency in the framework of the two-level nonlinear FAM with different coupling constants $\Gamma_1=0.25$ and $\Gamma_2=0.5$ for $\omega_0=1$, $\lambda_1=0.015$, and $\lambda_2=0.005$. The input amplitude $\phi_{in}=0.75$.

sider that $(\tilde{E}^2 - \epsilon^2)^2 \ll 4\Gamma^2\tilde{E}^2$ in Eqs. (15) to obtain

$$\begin{aligned} x\tilde{E} &\approx f(\tilde{E} - \epsilon)/2, \\ y\tilde{E} &\approx f(\tilde{E} + \epsilon)/2, \end{aligned} \quad (19)$$

where $x=\sqrt{X}=|A_1|$, $y=\sqrt{Y}=|A_2|$, and $f=\sqrt{P}/\Gamma=\phi_{in}/\sqrt{\Gamma}$. From here it follows that $x+y=f$.

The first case $\tilde{E}=\epsilon$ gives the following equation:

$$E - \omega_0 = \lambda_2(x - f)^2. \quad (20)$$

Moreover, we have from Eqs. (19) for $f \ll 1$

$$(\lambda_1 + \lambda_2)x^3 - 3\lambda_2fx^2 - 2Ex + f(E - \omega_0) \approx 0. \quad (21)$$

Combination of Eqs. (20) and (21) gives us

$$X \approx X_c - \frac{2\lambda_2\sqrt{X_c}}{\lambda_1 - \lambda_2}f. \quad (22)$$

Similarly, for the second case $\tilde{E}=-\epsilon$ we obtain

$$E + \omega_0 = \lambda_1(y - f)^2, \quad (23)$$

$$(\lambda_1 + \lambda_2)y^3 - 3\lambda_1fy^2 - 2Ey + f(E + \omega_0) \approx 0. \quad (24)$$

Correspondingly, we obtain from Eqs. (23) and (24)

$$Y \approx X_c + \frac{2\lambda_1\sqrt{X_c}}{\lambda_1 - \lambda_2}f. \quad (25)$$

Substituting Eqs. (22) and (25) into Eqs. (20) and (23), we obtain that the value of splitting of the BSC resonance equals

$$\Gamma_{BSC} \approx \frac{4\lambda_1\lambda_2}{\lambda_1 - \lambda_2} \left[\frac{2\omega_0}{\Gamma(\lambda_1 - \lambda_2)} \right]^{1/2} \phi_{in}. \quad (26)$$

As one can see from Figs. 5 and 6 the splitting of the BSC resonance is complemented by the splitting of the resonance width. Estimation (26) is in good agreement with numerics.

Finally, we present the transmission for the nonlinear FAM (3) with different coupling constants $\Gamma_1=0.25$ and $\Gamma_2=0.5$ (Fig. 7). Comparison to Figs. 2(a), 5(a), and 6(a) demonstrates that the choice $\Gamma_1=\Gamma_2$ is quite general. Also, one

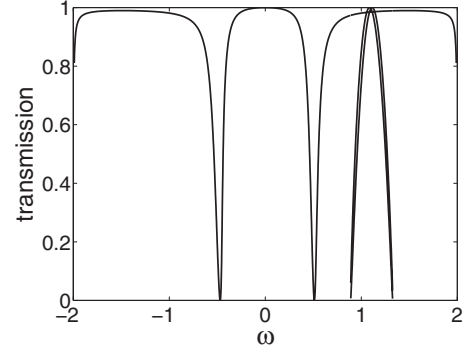


FIG. 8. The transmission $T=|t|^2/|\phi_{in}|^2$ of the tight-binding model (6) over the frequency calculated by formula (8) for $\omega_0=0.5$ and $u=0.3$. The nonlinear parameters are $\lambda_1=0.008$ and $\lambda_2=0.003$. The input amplitude $\phi_{in}=0.3$.

can see next from Fig. 8 that the tight-binding model (6) displays the same features in the transmission calculated by formula (8) as the two-level nonlinear FAM except that the model of the off-channel defects displays resonance dips instead of resonance peaks.²⁸

IV. DISCUSSION

Nonlinearity reveals important conceptual aspect of the bound states in the continuum. In the same way as nonlinearity makes the BSC observable in transmission, it should also cause the BSC to be only quasibound rather than bound as different from the linear model. One might therefore argue that the states which were the bound states in the continuum are actually not “BSCs” anymore in the nonlinear FAM. In fact, the situation crucially depends on both nonlinear non-zero coefficients λ_1, λ_2 , and on a value of the input amplitude ϕ_{in} . First, if the continuum is “empty,” i.e., there is no incident wave $\phi_{in}=0$, the coupled mode equations (3) have the homogeneous antisymmetric solution $A_1=-A_2$. Therefore, the solution is localized only at inner states of the impurity system. Thus, in that sense we can consider that the BSC exists by the same arguments as in the linear case. For the nonlinear FAM the BSC point is given by Eq. (16).

Next, one can see that the BSC solution $\begin{pmatrix} 1 \\ -1 \end{pmatrix}$ is orthogonal to the right part of the LS equation (1) or Eqs. (3) for $\Gamma_1=\Gamma_2$. If the model were linear we would write the general solution of the LS equation in the form of arbitrary linear superposition (5) (Ref. 25) in which the BSC participates independently of the incident wave. However, for transmission through nonlinear media we cannot write the general solution of the LS equations as a linear superposition of the BSC and the particular solution in form (5). The reason is obvious. The effective Hamiltonian in the LS equation (1) depends itself on this superposition. Therefore, the nonlinearity of the FAM model provides a coupling between the transmitted wave and the BSC. However, one can see that for variation in energy or frequency of the incident wave the populations of the impurity states go through the BSC point as Fig. 3(d) shows. Simultaneously at this point the imaginary part turns to zero as Fig. 4 shows. Thus, the BSC sur-

vives even under the effect of the input wave. However, that holds only if $\lambda_2=0$.

For the case where nonlinearity coefficients are not equal to zero, the BSC ceases to be bound even at the BSC energy as Figs. 5 and 6 show. For an evolution of the populations X and Y , we see from Fig. 5(d) that the BSC point is not reached except the case $P \rightarrow 0$. The resonance width becomes zero at those energies at which the transmission achieves a unit at the BSC induced resonance curve in Figs. 5(a) and 6(a) but not at $E=E_c$. Figure 6(c) shows that positions of resonances coincide there too. Then in view of linear theory, one could define these points as the BSC ones.^{14,15,33} How-

ever, in the nonlinear case a crossing of resonances or zero imaginary part of the complex eigenvalues of the effective Hamiltonian cannot serve as a signature of the BSC. Only for asymptotically small amplitude $\phi_{in} \rightarrow 0$ the quasibound BSC becomes real BSC.

ACKNOWLEDGMENTS

The work was partially supported by RFBR Grant No. 09-02-98005 "Siberia." We thank Dima Maksimov for remarks and Kostya Pichugin for discussions.

-
- ¹J. von Neumann and E. Wigner, Phys. Z. **30**, 465 (1929).
²F. H. Stillinger and D. R. Herrick, Phys. Rev. A **11**, 446 (1975).
³D. R. Herrick, Physica B & C **85**, 44 (1976).
⁴F. H. Stillinger, Physica B & C **85**, 270 (1976).
⁵F. Capasso, C. Sirtori, J. Faist, D. L. Sivco, Sung-Nee G. Chu, and A. Y. Cho, Nature (London) **358**, 565 (1992).
⁶S. Longhi, Eur. Phys. J. B **57**, 45 (2007).
⁷A. F. Sadreev, E. N. Bulgakov, K. N. Pichugin, I. Rotter, and T. V. Babushkina, in *Quantum Dots, Research, Technology and Applications*, edited by R. W. Knoss (Nova Science Publishers, Hauppauge, NY, 2008), pp. 547–577.
⁸N. Moiseyev, Phys. Rev. Lett. **102**, 167404 (2009).
⁹S. Fan, P. R. Villeneuve, J. D. Joannopoulos, and H. A. Haus, Phys. Rev. Lett. **80**, 960 (1998).
¹⁰E. N. Bulgakov and A. F. Sadreev, Phys. Rev. B **78**, 075105 (2008).
¹¹D. C. Marinica, A. G. Borisov, and S. V. Shabanov, Phys. Rev. Lett. **100**, 183902 (2008).
¹²A. Miroshnichenko, S. Flach, and Y. Kivshar, arXiv:0902.3014 (unpublished).
¹³H. Feshbach, Ann. Phys. (N.Y.) **5**, 357 (1958).
¹⁴A. Z. Devdariani, V. N. Ostrovsky, and Yu. N. Sebyakin, Sov. Phys. JETP **44**, 477 (1976).
¹⁵H. Friedrich and D. Wintgen, Phys. Rev. A **32**, 3231 (1985).
¹⁶A. Volya and V. Zelevinsky, Phys. Rev. C **67**, 054322 (2003).
¹⁷A. F. Sadreev, E. N. Bulgakov, and I. Rotter, Phys. Rev. B **73**, 235342 (2006).
¹⁸U. Fano, Phys. Rev. **124**, 1866 (1961).
¹⁹P. W. Anderson, Phys. Rev. **124**, 41 (1961).
²⁰I. Rotter, Rep. Prog. Phys. **54**, 635 (1991).
²¹A. F. Sadreev and I. Rotter, J. Phys. A **36**, 11413 (2003).
²²Z. Wang and S. Fan, Phys. Rev. E **68**, 066616 (2003).
²³J. Joannopoulos, S. G. Johnson, J. N. Winn, and R. D. Meade, *Photonic Crystals: Molding the Flow of Light* (Princeton University Press, Princeton, NJ, 2008).
²⁴C. S. Kim, A. M. Satanin, Y. S. Joe, and R. M. Cosby, Phys. Rev. B **60**, 10962 (1999).
²⁵E. N. Bulgakov, K. N. Pichugin, A. F. Sadreev, and I. Rotter, JETP Lett. **84**, 430 (2006).
²⁶M. I. Molina and G. P. Tsironis, Phys. Rev. B **47**, 15330 (1993).
²⁷A. R. McGurn and G. Birkok, Phys. Rev. B **69**, 235105 (2004).
²⁸A. E. Miroshnichenko, S. F. Mingaleev, S. Flach, and Yu. S. Kivshar, Phys. Rev. E **71**, 036626 (2005).
²⁹S. Longhi, Phys. Rev. B **75**, 184306 (2007).
³⁰K. Busch, S. F. Mingaleev, A. Garcia-Martin, M. Schillinger, and D. Hermann, J. Phys.: Condens. Matter **15**, R1233 (2003).
³¹A. R. McGurn, Adv. Optoelectron. **2007**, 92901 (2007); Phys. Rev. B **77**, 115105 (2008).
³²S. Mingaleev and Y. Kivshar, J. Opt. Soc. Am. B **19**, 2241 (2002).
³³E. N. Bulgakov, I. Rotter, and A. F. Sadreev, Phys. Rev. A **75**, 067401 (2007).